E-cigarette vapor renders neutrophils dysfunctional due to filamentous actin accumulation

Jasper, Alice; Faniyi, Aduragbemi; Davis, Lauren; Grudzinska, Frances; Halston, Robyn; Hazeldine, Jon; Parekh, Dhruv; Sapey, Elizabeth; Thickett, David; Scott, Aaron

DOI:
10.1016/j.jaci.2023.08.025

E-cigarette vapor renders neutrophils dysfunctional due to filamentous actin accumulation

Alice E. Jasper, PhD,[a] Aduragbemi A. Faniyi, PhD,[a] Lauren C. Davis, PhD,[a] Frances S. Grudzinska, MRes,[a] Robyn Halston, MSc,[a] Jon Hazeldine, PhD,[b] Dhruv Parekh, PhD,[a,c,e] Elizabeth Sapey, PhD,[a,d,e] David R. Thickett, MD,[a,e] and Aaron Scott, PhD[a,e] *Birmingham, United Kingdom*

Background: Electronic cigarette (e-cigarette) use continues to rise despite concerns of long-term effects, especially the risk of developing lung diseases such as chronic obstructive pulmonary disease. Neutrophils are central to the pathogenesis of chronic obstructive pulmonary disease, with changes in phenotype and function implicated in tissue damage.

Objective: We sought to measure the impact of direct exposure to nicotine-containing and nicotine-free e-cigarette vapor on human neutrophil function and phenotype.

Methods: Neutrophils were isolated from the whole blood of self-reported nonsmoking, nonvaping healthy volunteers. Neutrophils were exposed to 40 puffs of e-cigarette vapor generated from e-cigarette devices using flavorless e-cigarette liquids with and without nicotine before functions, deformability, and phenotype were assessed.

Results: Neutrophil surface marker expression was altered, with CD62L and CXCR2 expression significantly reduced in neutrophils treated with e-cigarette vapor containing nicotine. Neutrophil migration to IL-8, phagocytosis of *Escherichia coli* and *Staphylococcus aureus* pHrodo bioparticles, oxidative burst response, and phorbol 12-myristate 13-acetate–stimulated neutrophil extracellular trap formation were all significantly reduced by e-cigarette vapor treatments, independent of nicotine content. E-cigarette vapor induced increased levels of baseline polymerized filamentous actin levels in the cytoplasm, compared with untreated controls.

Conclusions: The significant reduction in effector neutrophil functions after exposure to high-power e-cigarette devices, even in the absence of nicotine, is associated with excessive filamentous actin polymerization. This highlights the potentially damaging impact of vaping on respiratory health and reinforces the urgency of research to uncover the long-term health implications of e-cigarettes. (J Allergy Clin Immunol 2024;153:320-9.)

Key words: *Neutrophils, e-cigarettes, nicotine, phagocytosis, NETosis, oxidative burst*

Electronic cigarettes (e-cigarettes) were designed to reduce the harm caused by tobacco smoking. In 2021, the Global State of Tobacco Harm Reduction project estimated that there were 82 million e-cigarette users worldwide.[1] The use of e-cigarettes, particularly disposable devices, continues to rise rapidly in popularity among young people and adults alike, despite uncertainties about their long-term safety.[2]

In the developed world, smoking is the most common risk factor for developing chronic obstructive pulmonary disease (COPD) and increases the risk of emphysema, recurrent infection, and lung cancer. Neutrophils play an essential role in inflammation initiation and resolution and are rapidly recruited to sites of inflammation and tissue injury. In COPD, airway neutrophilia is directly correlated with the severity of airflow obstruction, the rate of decline in lung physiology, and the progression of emphysema.[3-7] Cigarette smoke–induced neutrophil dysfunction has been causally associated with tissue damage, small airways disease, exacerbation frequency, and mortality after COPD diagnosis.[3] Furthermore, neutrophil dysfunction after *in vitro* cigarette smoke exposure mimics that reported in patients with COPD.[8,9] Neutrophils are also implicated in other lung diseases, for example, interstitial lung disease in which bronchoalveolar lavage neutrophilia is associated with disease severity and poor prognosis.[10,11] Although the effects of smoking on neutrophil function can be induced following both acute and chronic exposures, smoking-related lung damage is slowly progressive, taking years to become clinically discernible. Given the relative youth of e-cigarette research, the relationship between vaping and inflammatory lung disease remains unclear.

Before the addition of nicotine and/or flavoring agents, e-cigarette liquids (e-liquids) consist of the base elements propylene glycol (PG) and vegetable glycerine (VG), which are generally regarded as safe for human consumption by the US Food and Drug Administration. However, when these components are vaporized, the chemical composition changes and they

From [a]the Birmingham Acute Care Research Group, Institute of Inflammation and Ageing, University of Birmingham, [b]the National Institute for Health Research Surgical Reconstruction and Microbiology Research Centre, Queen Elizabeth Hospital Birmingham, [c]the NIHR Clinical Research Facility, University Hospitals Birmingham NHS Foundation Trust, Edgbaston, [d]the PIONEER HDR-UK Hub in Acute Care, Institute of Inflammation and Ageing, University of Birmingham, and [e]the National Institute for Health and Care Research (NIHR) Birmingham Biomedical Research Centre, Institute of Translational Medicine, Birmingham.

Received for publication May 12, 2023; revised July 23, 2023; accepted for publication August 18, 2023.

Available online September 5, 2023.

Corresponding author: Aaron Scott, PhD, National Institute for Health and Care Research (NIHR) Birmingham Biomedical Research Centre, Institute of Translational Medicine, Birmingham, B152TH, UK. E-mail: a.scott@bham.ac.uk.

0091-6749

https://doi.org/10.1016/j.jaci.2023.08.025

Abbreviations used
COPD: Chronic obstructive pulmonary disease
FITC: Fluorescein isothiocyanate
MFI: Median fluorescence intensity
NET: Neutrophil extracellular trap
PG: Propylene glycol
PMA: Phorbol myristate acetate
RCS: Reactive carbonyl species
ROS: Reactive oxygen species
VG: Vegetable glycerine
XF: Extracellular flux

produce reactive carbonyl species (RCS) such as formaldehyde, acetaldehyde, and acrolein,[12-15] which are also found in cigarette smoke.

Research has focused on cellular effects of e-cigarette vapor to detect changes predictive of long-term outcomes. Dysregulated neutrophil migration, phagocytosis, protein secretion, formation of neutrophil extracellular traps (NETosis), and reactive oxygen species (ROS) generation have been reported.[16-18] Neutrophils are highly glycolytic cells, and glycolytic inhibitors have been shown to abolish neutrophil functions,[19] but glycolysis has not been investigated in the context of e-cigarette–induced dysfunction. The ability of neutrophils to rearrange filamentous actin (F-actin) to polarize and direct migration has been demonstrated to be impaired by e-cigarette vapor extract,[16] but the contribution of baseline deformability to neutrophil dysfunction has not been explored despite its importance in effector functions. Existing studies are limited by the use of e-cigarette vapor condensate or vapor extract models, which heavily dilute and may fail to capture some vapor constituents.

Here, using both nicotine-containing and nicotine-free e-liquid formulations, we have used a direct model of e-cigarette vapor exposure to investigate its impact on human neutrophil phenotype and function. We aimed to determine whether e-cigarette–induced changes in phenotype and function could be attributed to changes in glycolytic function or cell deformability. Understanding the effect of e-cigarettes on neutrophil function and the underlying driving mechanisms will help to predict the likelihood of e-cigarette users developing features of smoking-related lung diseases after long-term use.

METHODS

Detailed methodology can be found in the Methods section in this article's Online Repository at www.jacionline.org. All studies were undertaken following ethical approvals, which were provided by the University of Birmingham Research Ethics Committee (ERN 12-1185R2). Written informed consent was obtained from all participants before the collection of data and biological samples.

Study subjects

Volunteers were recruited from members of staff at the University of Birmingham Research Laboratories in the Queen Elizabeth Hospital Birmingham (age range, 19-63 years; 17 female and 14 male participants). Participants were self-reported never-smokers, never-vapers, and otherwise healthy as defined by the absence of chronic or acute medical conditions and by taking no regular prescription medications.

Materials

All materials were purchased from Merck (Gillingham, Dorset, UK), unless stated otherwise.

Isolation of peripheral blood neutrophils

Neutrophils were isolated from lithium-heparin anticoagulated venous blood via discontinuous Percoll gradient separation technique as described previously.[20,21] Postisolation, neutrophils were resuspended at 1×10^6/mL in sterile RPMI containing 2 mM L-glutamine, supplemented with 1% (vol/vol) penicillin-streptomycin.

E-cigarette devices

KangerTech TOPBOX mini (modifiable parameters, set to 315ºC, 0.2 Ω, 75 W) e-cigarette starter kits (Amazon, Manchester, UK) and KangerTech replacement atomizers (Amazon) were loaded with flavorless e-liquid (50:50 [PG:VG]) containing 0 or 36 mg/mL nicotine (maximum strength on the market at the time of project conception) (American e-liquid). A fully charged battery (rechargeable 3000 mAh, 3.7 V) and a filled tank (allowing time for the wick to saturate to prevent dry puffs) were used each time, and atomizers were changed regularly.

E-cigarette vapor chamber

A modified hypoxia chamber (total volume, 5.5 L) was used as an e-cigarette vapor exposure system. The chamber was attached to a vacuum pump to generate the suction required for full e-cigarette activation. Every 30 seconds, the e-cigarette was activated manually via the activating switch, at the same time as the vacuum started, creating a puff in the chamber lasting 4 seconds (duration based on topography studies[22-25]). A 30-second interpuff interval allowed the device to cool between puffs to prevent overheating. A total of 40 puffs were generated over a 20-minute period.

Neutrophil functional and phenotypic assays

Neutrophils (1×10^5) were plated into a 96-well flexi-plate (Corning, Loughborough, UK) precoated with PBS containing 1% BSA and placed in the center of the e-cigarette vapor chamber (except during chemotaxis assays when cells were exposed while adhered to coverslips). After e-cigarette vapor exposure, phenotypical and functional analyses were performed as described in the Online Repository.

Statistical analysis

All statistical analyses were performed using GraphPad Prism (version 9.0.2 for Mac, Dotmatics, Boston, Mass). A normality test (Shapiro-Wilk test) was carried out on all data sets. Repeated-measures ANOVA (for normally distributed data) and the Kruskal-Wallis/Friedman tests (for not normally distributed data) were used. A P value of less than or equal to .05 was considered statistically significant.

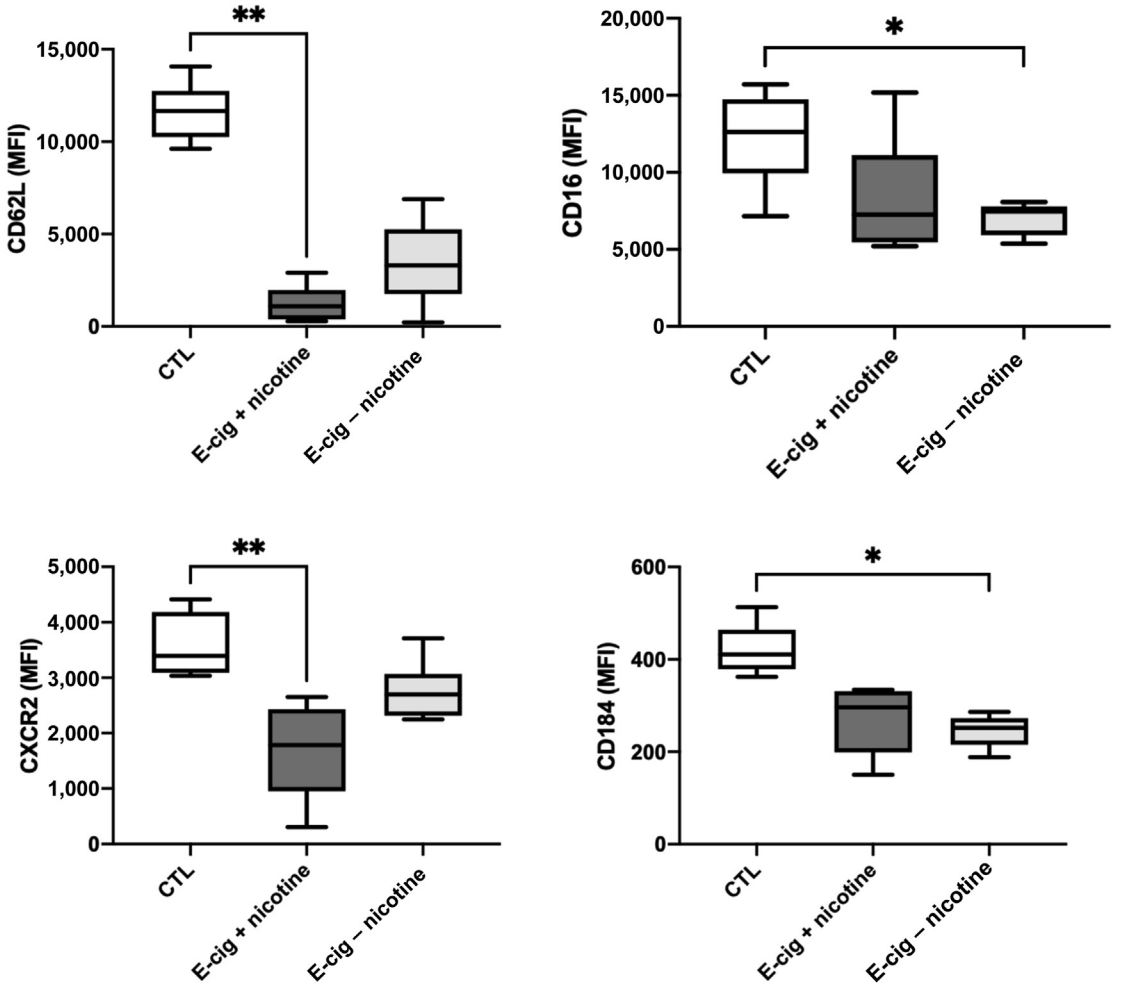

FIG 1. Neutrophil surface marker phenotyping after e-cigarette vapor exposure. Expression of 11 surface markers was measured after e-cigarette treatment using a multicolor panel and analyzed using a flow cytometer. Cell surface marker expression is presented as MFI. Statistical significance was assessed using the Friedman test. A significant difference between treatment groups is indicated by asterisks above a capped line between the 2 statistically different groups. *CTL*, Untreated control. $*P \leq .05$; $**P \leq .01$; (n = 6).

Data sharing

To access original data presented in this manuscript, please contact the corresponding author: a.scott@bham.ac.uk.

RESULTS

Neutrophil phenotypic markers are altered in response to e-cigarette vapor exposure

Forty puffs of e-cigarette vapor had no significant effect on neutrophil viability immediately after exposure or after 24 hours (see Fig E1 in this article's Online Repository at www.jacionline.org). Using this nontoxic puff regimen, we examined the impact of e-cigarette vapor on neutrophil cell surface marker expression.

Neutrophils exposed to e-cigarette vapor containing nicotine exhibited a 90.6% reduction in the median fluorescence intensity (MFI) of CD62L compared with untreated controls ($P = .0045$; Fig 1, *A*). There was no difference in CD62L expression after treatment with nicotine-free vapor. There was a trend toward reduced MFI of CD16 for neutrophils treated with nicotine-containing e-cigarette vapor ($P = .0628$). Exposure to nicotine-free vapor reduced CD16 expression by 40.8% ($P = .0117$; Fig 1, *B*).

Neutrophil CXCR2 expression was reduced by 47.4% ($P = .0045$; Fig 1, *C*) when treated with nicotine-containing vapor, but not with nicotine-free vapor ($P = .0628$).

There was a trend toward a reduction in the MFI of CD184 in neutrophils treated with nicotine-containing e-cigarette vapor ($P = .0628$). However, when treated with nicotine-free e-cigarette vapor, CD184 expression was reduced by 38.7% ($P = .0117$; Fig 1, *D*). There was a trend toward a reduction in MFI of CD11c in neutrophils treated with nicotine-containing e-cigarette vapor ($P = .0628$), and this was significantly reduced by 16.8% ($P = .0117$) in neutrophils exposed to nicotine-free e-cigarette vapor (Fig E1, *B*).

No significant changes were observed in the expression of PD-L1, CD10, CD54, CD11b, or CD66b following treatment with nicotine-containing or nicotine-free e-cigarette vapor (see Fig E2 in this article's Online Repository at www.jacionline.org).

E-cigarette vapor slows neutrophil chemotaxis and transmigration to IL-8 (CXCL8)

Exposure to nicotine-containing and nicotine-free e-cigarette vapor significantly reduced neutrophil transmigration, with the

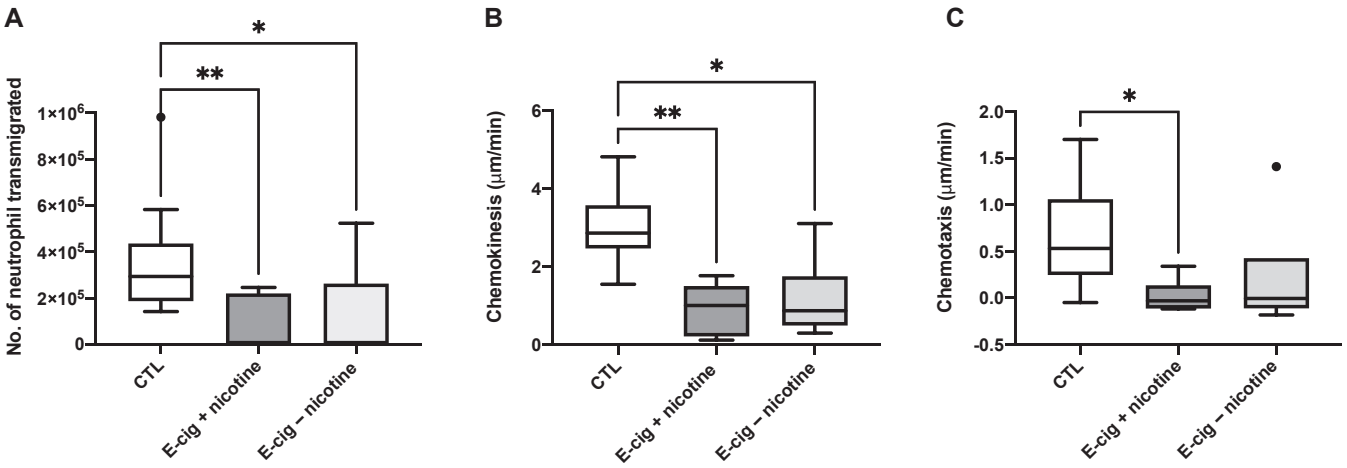

FIG 2. E-cigarette vapor reduces neutrophil migration to 100 nM IL-8. **A,** Neutrophil transmigration across a membrane toward 100 nM IL-8 was assessed over a 90-minute period following e-cigarette treatment. **B** and **C,** Neutrophil speed (Fig 2, *B*) and velocity (Fig 2, *C*) of migration to 100 nM IL-8 were assessed using an Insall chamber and video microscope as described. Data were not normally distributed, and so the Kruskal-Wallis test was performed to assess statistical difference. *CTL*, Untreated control. $*P \leq .05$; $**P \leq .01$; (Fig 2, *A*, n = 10; Fig 2, *B* and *C*, n = 6).

total number of neutrophils that had migrated toward CXCL8 reduced by 77.4% ($P = .0032$) and 66.6% ($P = .0203$), respectively, when compared with untreated controls (Fig 2, *A*).

Analysis of chemotactic dynamics using the Insall chamber revealed that treatment with e-cigarette vapor containing nicotine reduced neutrophil chemokinesis to CXCL8 by 76.3% ($P = .0058$; Fig 2, *B*). Chemokinesis was reduced by 85.5% ($P = .0152$) when neutrophils were treated with nicotine-free e-cigarette vapor. Neutrophil velocity (chemotaxis) was reduced by 114.8% ($P = .0433$) after treatment with nicotine-containing e-cigarette vapor (Fig 2, *C*). In contrast, nicotine-free vapor had no effect on neutrophil chemotaxis.

E-cigarette vapor inhibits neutrophil phagocytosis of *Escherichia coli* and *Staphylococcus aureus* bioparticles

Neutrophil phagocytosis of *E coli* and *S aureus* pHrodo bioparticles was assessed at 30 minutes during intermediate-phase phagocytosis. Compared with untreated controls, the proportion of *E coli*–positive neutrophils was reduced by 94.4% ($P = .0060$) and 97.9% ($P = .0026$) following treatment with nicotine-containing and nicotine-free e-cigarette vapor, respectively (Fig 3, *A*). The proportion of *S aureus*–positive neutrophils was reduced by 93.3% ($P = .0044$; Fig 3, *B*) after treatment with nicotine-containing e-cigarette vapor and reduced by 92.2% ($P = .0021$; Fig 3, *B*) after nicotine-free vapor treatment, compared with controls.

To determine whether this reduction in phagocytosis was a consequence of a reduced maximal capacity to phagocytose or a slower rate of phagocytosis, neutrophils were also incubated with *E coli* and *S aureus* for 60 minutes.

Compared with controls, treatment with nicotine-containing e-cigarette vapor reduced the proportion of *E coli* bioparticle–positive neutrophils by 96.2% ($P = .0157$) compared with a 98.0% ($P = .0034$; Fig 3, *C*) reduction when nicotine-free vapor was used. Compared with untreated controls, treatment with nicotine-containing and nicotine-free e-cigarette vapor reduced the proportion of *S aureus* bioparticle–positive neutrophils by 94.4% ($P = .0044$) and 91.0% ($P = .0021$), respectively (Fig 3, *D*).

Phorbol myristate acetate–stimulated NET generation is impaired by e-cigarette vapor exposure

Neutrophil capacity for NETosis after e-cigarette vapor exposure was determined by a fluorescence-based assay with confirmation by microscopy. E-cigarette vapor did not induce spontaneous NETosis, as shown in Fig 4, *A*. In response to stimulation with 25 nM phorbol myristate acetate (PMA), the magnitude of NET response mounted to PMA was calculated (stimulated − unstimulated). Compared with untreated controls, neutrophils treated with e-cigarette vapor containing nicotine exhibited an 86.0% ($P = .0226$; Fig 4, *C*) reduction in the NET response mounted to PMA. When nicotine-free e-cigarette vapor was used to treat neutrophils, the NET response mounted to PMA remained suppressed by 89.9% ($P = .0099$; Fig 4, *B*). Immunofluorescence imaging of NET generation revealed that neutrophils treated with e-cigarette vapor did not undergo nuclear decondensation (Fig 4, *C*).

E-cigarette vapor impairs oxidative burst response in neutrophils

Oxidative burst after 160 nM PMA stimulation was assessed using extracellular flux (XF) technology, with oxygen consumption rate used as a surrogate marker of ROS generation. The area under the curve during the oxidative burst response, expressed as the total oxygen consumption, was reduced by 76.9% ($P = .0281$; Fig 5, *A* and *B*) for neutrophils pretreated with e-cigarette vapor containing nicotine when compared with controls. When nicotine was absent from the e-cigarette vapor, oxidative burst response was reduced by 64.3% ($P = .0281$; Fig 5, *A* and *B*).

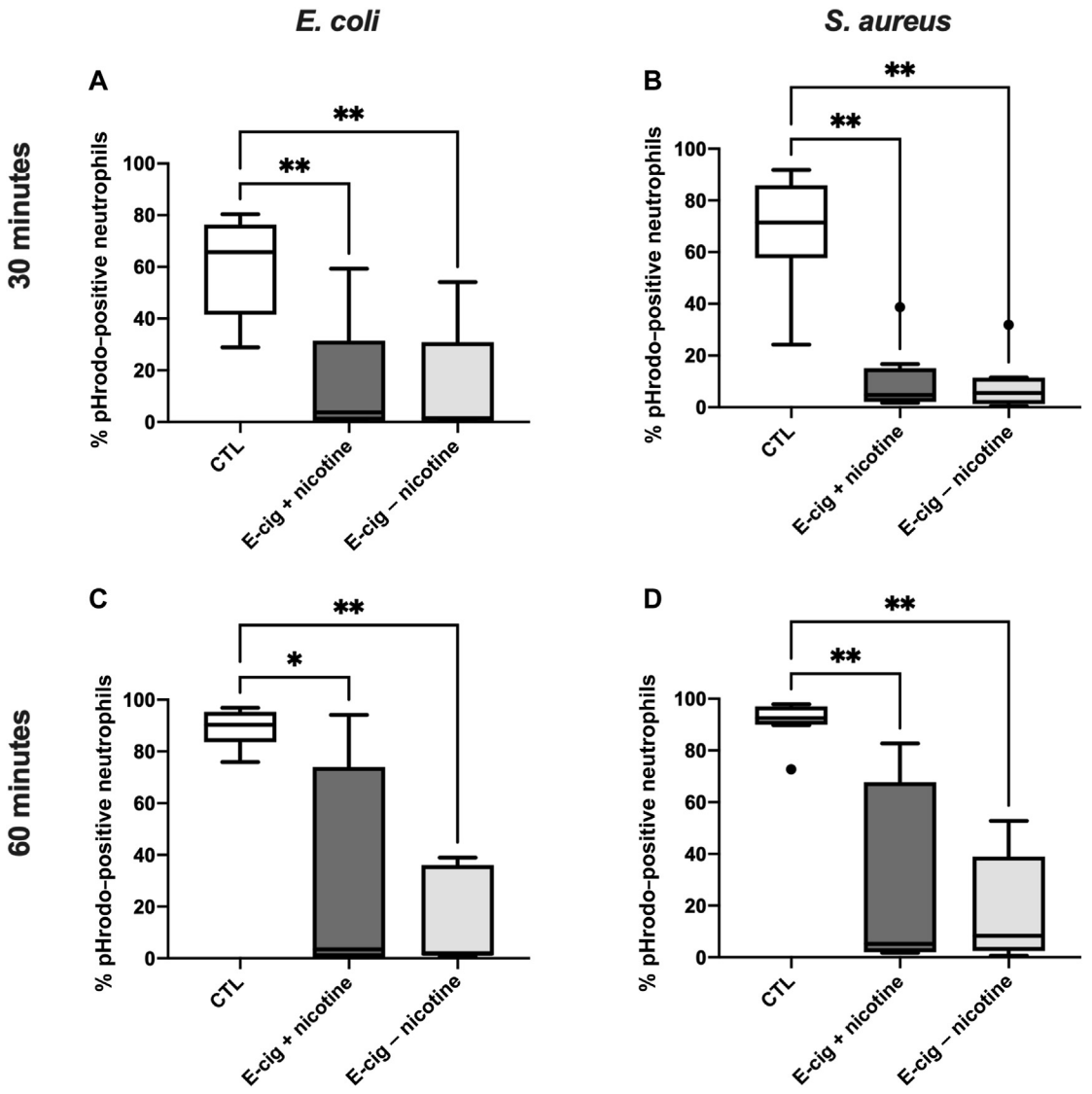

FIG 3. E-cigarette vapor reduces neutrophil phagocytosis of *E coli* and *S aureus* pHrodo bioparticles. Neutrophils were treated with relevant e-cigarette vapor before incubation with *E coli* (Fig 3, *A* and *C*) or *S aureus* (Fig 3, *B* and *D*) pHrodo bioparticles for 30 (Fig 3, *A* and *B*) or 60 (Fig 3, *C* and *D*) minutes. The percentage of pHrodo-positive cells in the population was recorded (on the basis of cytochalasin D–negative control samples). Data were not normally distributed, and so statistical significance was assessed using the Kruskal-Wallis test. *CTL*, Untreated control. $*P \leq .05$; $**P \leq .01$; (n = 9).

In addition to XF analysis, cytoplasmic and mitochondrial ROS production was measured using the CellROX fluorescent dye. There was a trend toward a reduction in cytoplasmic ROS levels in neutrophils treated with nicotine-containing e-cigarette vapor ($P = .0628$) compared with controls and a 94.8% ($P = .0051$) reduction when nicotine-free vapor was used. Similarly, there was a trend toward a reduction in mitochondrial/nuclear ROS levels in neutrophils treated with e-cigarette vapor containing nicotine ($P = .0911$) and levels were 84.2% ($P = .0022$) lower after nicotine-free vapor treatment (Fig 5, *D*).

Neutrophil glycolysis is not impaired by e-cigarette vapor exposure

Using an XF analyzer, we assessed basal and stimulated glycolysis of neutrophils exposed to e-cigarette vapor to determine whether changes in metabolism driven by e-cigarette exposure are associated with the observed dysfunction. After exposure to nicotine-containing and nicotine-free e-cigarette vapor, there were no differences in basal glycolysis (Fig 6, *A* and *B*), PMA-induced glycolysis (Fig 6, *A* and *C*), or glycolytic response to PMA (Fig 6, *A* and *D*).

E-cigarette vapor exposure increases baseline F-actin polymerization in neutrophils

As a marker of neutrophil deformability, we examined F-actin polymerization in neutrophils stained with fluorescein isothiocyanate (FITC)-conjugated phalloidin, which binds to the polymerized F-actin, but not its monomeric form. Fig 7, *A*, shows representative microscopy images of neutrophils treated with e-cigarette vapor. Fluorescence intensity increased after e-cigarette

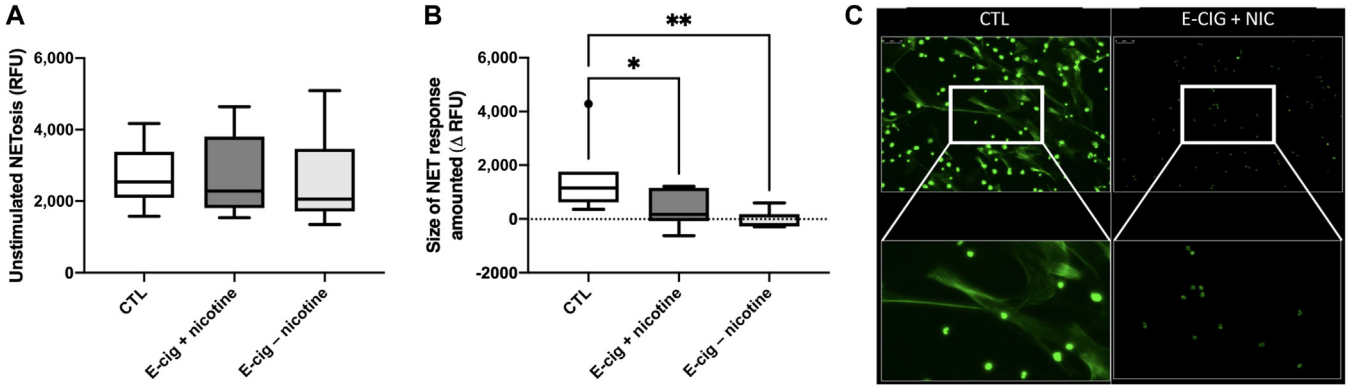

FIG 4. E-cigarette vapor reduces PMA-stimulated NETosis. Neutrophil NETosis was measured using SYTOX Green dye, as described. Fluorescence was measured using a plate reader, and the RFU readout correlates with NET generation. NETosis was assessed after exposure to e-cigarette vapor, with or without stimulation with 25 nM PMA. Unstimulated NETosis (**A**) and the size of the NET response to PMA (PMA-stimulated − unstimulated = ΔRFU) (**B**) were measured. Values were corrected to baseline. **C,** In addition, NETs were assessed by immunofluorescence staining using SYTOX Green. The Friedman test was performed to assess statistical differences. *CTL*, Untreated control; *RFU*, relative fluorescence unit. $*P \leq .05$, $**P \leq .01$ (n = 8 per group).

vapor exposure, suggesting higher levels of baseline polymerized F-actin in the cell cytoplasm. Neutrophils exhibited a 42.8% ($P = .0237$) and a 43.5% ($P = .0360$) increase in baseline F-actin levels when treated with nicotine-containing and nicotine-free e-cigarette vapor, respectively (Fig 7, *B*). Neutrophils with lower baseline F-actin transmigrated more ($R^2 = 0.2154$; $P = .0169$; Fig 7, *C*) than those with high baseline levels of F-actin, implicating accumulation of F-actin in the e-cigarette–induced dysfunction of neutrophils.

PD-L1 expression was the only measurement with a significant difference between nicotine-free and nicotine-containing treatment groups. All measurements, including median values, interquartile ranges, and *P* values for all tests performed in this study, are provided in Table E1 (in the Online Repository available at www.jacionline.org).

DISCUSSION

Direct treatment with e-cigarette vapor induced significant dysfunction in neutrophils, and this was associated with changes in cell surface markers involved in environment sensing and adhesion. These replicate some of the phenotypic and functional changes seen in neutrophils from patients with COPD, such as reduced chemokinesis[7] and reduced NETosis,[26] and may increase tissue damage, susceptibility to infection, and inflammation after long-term e-cigarette use. The global neutrophil effector dysfunction following direct e-cigarette vapor treatment is a feature that suggests the involvement of a central cellular pathway. Therefore, we investigated metabolism but did not find a difference in glycolysis, suggesting that this was not a driver of the dysfunction seen. Then, we considered which core pathway is shared by phagocytosis, migration, and NETosis and could be induced by known constituents of e-cigarette vapor. We found F-actin, a molecule implicated in cell deformability, to be a potential driver of dysfunction seen. Notable F-actin expression correlated negatively with cellular migration, suggesting a relationship between the two. The relationship between migration, a process that requires rearrangement of the cytoskeleton for the formation of pseudopods, and F-actin polymerization was assessed as a proof-of-concept study. Other functions, including phagocytosis and NETosis, require similar F-actin dynamics.[27] This therefore suggests that this mechanism is likely to be implicated broadly across all effector functions.

Our data suggest that neutrophil dysfunction following e-cigarette exposure is driven by a reduction in deformability, thus physically arresting the rearrangement of the cell to exert effector functions. Reduced neutrophil deformability, and the associated inability to deprime, has also been recognized as a hallmark feature in acute lung injury.[28] We have demonstrated that polymerized F-actin is increased in neutrophils treated with e-cigarette vapor compared with untreated counterparts. Consistent with our findings, excessive actin polymerization has been shown to contribute to the inability of neutrophils to migrate after e-cigarette vapor extract exposure[16] and has been used as a surrogate marker for neutrophil deformability.[29] F-actin polymerization is an essential process in the formation of lamellipodia during chemotaxis and phagocytosis.[30] Increased F-actin polymerization prevents neutrophils rearranging the cytoskeleton and cell surface membrane, disrupting the ability of neutrophils to degranulate, to apoptose, and to assemble Nicotinamide adenine dinucleotide phosphate (NADPH) oxidase. Therefore, F-actin polymerization has consequences for all neutrophil functions and can explain the demonstrated cellular effects of e-cigarette vapor.

F-actin polymerization is not the only important process relating to F-actin. The ability to depolymerize F-actin is also essential, with depolymerization blockade abolishing neutrophil transmigration.[31] Evidence suggests that F-actin depolymerization is controlled by regulation of intracellular calcium levels,[32] and calcium signaling dysregulation has been hypothesized as a driving mechanism of e-cigarette–induced neutrophil dysfunction.[33] Therefore, F-actin polymerization may be the missing link between e-cigarette–induced neutrophil dysfunction and the reported changes in calcium signaling as a driving mechanism. Both calcium signaling and F-actin polymerization are processes that happen within minutes, and therefore could explain the rapid change in function seen after such an acute exposure of e-cigarette vapor. In concert, direct protein carbonylation caused by RCS and indirect via by-products of lipoxidation (4-hydroxynonenal) may drive the accumulation of F-actin observed

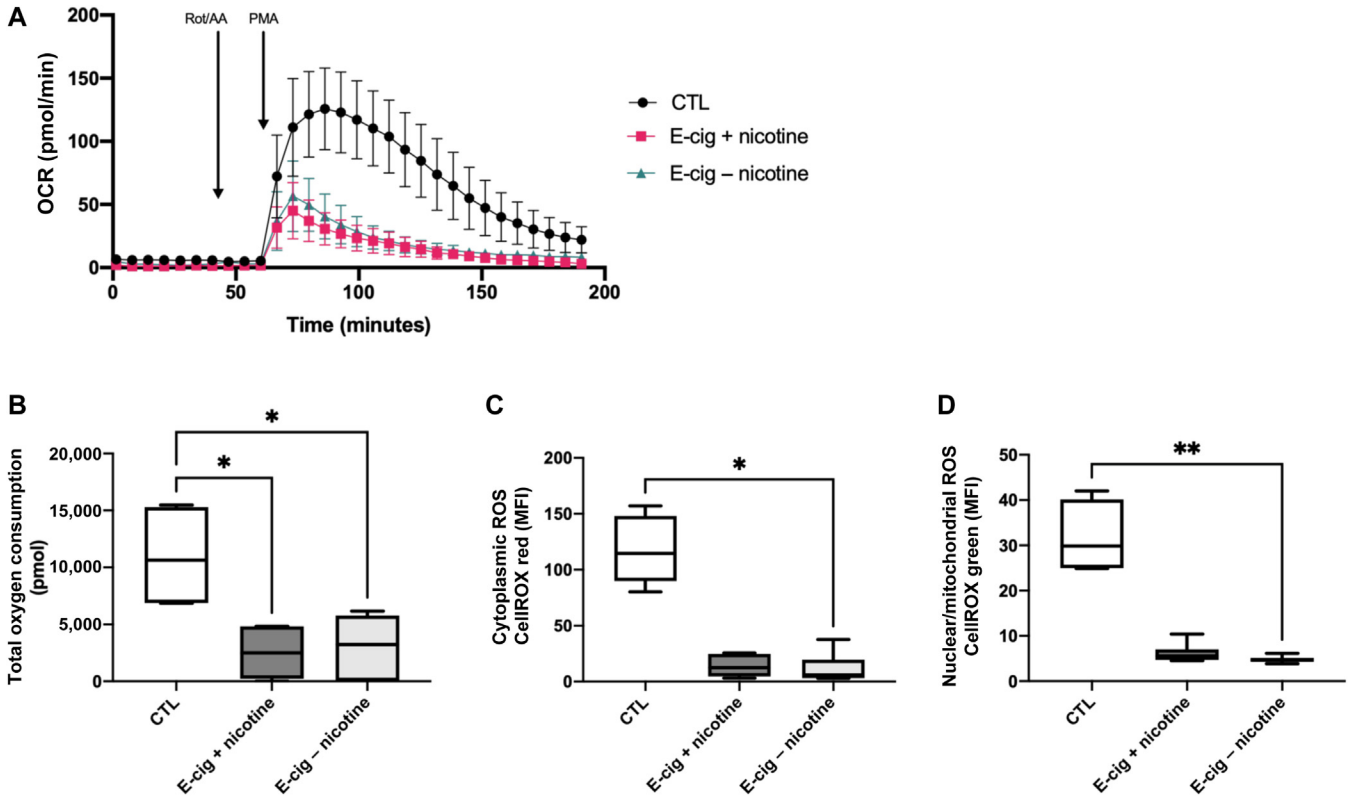

FIG 5. E-cigarette vapor reduces neutrophil oxidative burst and ROS production. Neutrophil oxidative burst response to 160 nM PMA was assessed using XF analyzers as described. **A,** The combined OCR trace for the duration of the metabolic test presented as mean ± SEM of 7 distinct donors. **B,** Area under the curve analysis was performed on the trace for each individual and the total oxygen consumption was calculated. **C** and **D,** In addition, neutrophils were stained using CellROX red (Fig 5, *C*) and CellROX green (Fig 5, *D*) to represent cytoplasmic and nuclear/mitochondrial ROS production. The Friedman test was used to assess statistical differences. Statistical significance is indicated by asterisks above each group, corresponding to a significant difference from CTL. *CTL*, Untreated control; 2-*DG*, 2-Deoxy-D-glucose; *OCR*, oxygen consumption rate. $*P \leq .05$; $**P \leq .01$; (n = 7).

after e-cigarette exposure. The RCS component in cigarette smoke can cause significant nonenzymatic posttranslational modification to proteins. Once exposure exceeds the ability of the cell to neutralize these potential oxidants, modification of proteins by oxidation results in targeting peptide residues such as Lys, Arg, His, and Cys.[34,35] We speculate that Cys18 on the p-loop of RAC1, of which the thiol side chain plays a role in stabilizing nucleotide binding, can be oxidized by the excessive RCS load present during e-cigarette vapor challenge. This results in effective constitutive activation of RAC1, which paradoxically leads to impaired membrane polarization and accumulation of F-actin in other cell types.[36]

Previous work has suggested that e-cigarettes activate neutrophils, with upregulation of CD11b and CD66b, morphological changes, proteinase secretion, and stimulated NET sensitivity.[17,18,33] We propose that these cellular effects cannot be attributed to neutrophil activation; typically, activation would upregulate function. Studies by Reidel and Ghosh examined neutrophils from chronic e-cigarette users, whereas the Higham study modeled a longer exposure than topography studies suggest.[22-25]

Neutrophils rapidly shed CD62L in response to infectious or inflammatory stimuli (see Table E2 in this article's Online Repository at www.jacionline.org), with reported values of up to 50% reduction following N-Formylmethionyl-leucyl-phenylalanine (fMLP) challenge.[37,38] Shedding of CD62L following e-cigarette vapor exposure is more pronounced, with a 90% reduction in expression appearing more comparable with cigarette smoke extract exposure than with traditional inflammatory stimuli.[39]

Together, these results may not represent differential hypotheses, but a biphasic neutrophil response whereby, despite rapid shedding of CD62L, acute exposure of neutrophils significantly arrests function because of reduced deformability. Chronic exposure as seen modeled with *in vivo* models may result in increased adaptive changes to neutrophil function before egress from the bone marrow. This could explain effects such as upregulation of degranulation, NETosis, and activation markers seen with *in vivo* models. The difference between these studies in terms of exposure time, nicotine level, energy input of device, and flavorings (if any) included in the liquids used will all have an impact on function and observed results and so must be taken into consideration.

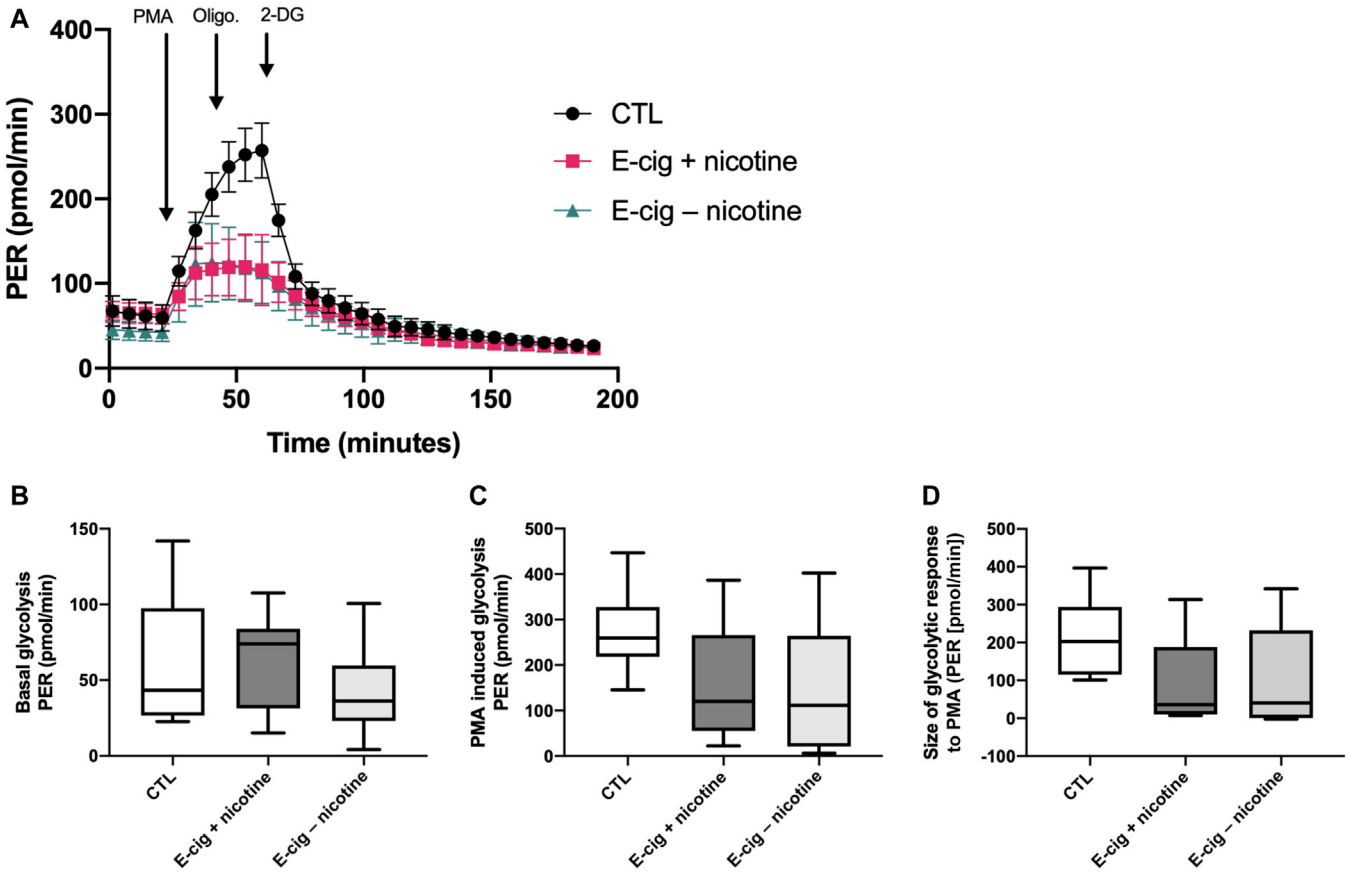

FIG 6. Neutrophil glycolysis test after exposure to e-cigarette vapor (XF injections: A, 160 nM PMA; B, 16 mM Oligo; and C, 500 mM 2-DG were used to assess glycolysis). **A,** The combined PER trace from 8 distinct donors. **B,** Basal glycolysis was measured as the final PER value before PMA injection. **C,** PMA-induced glycolysis was the maximum PER reached across the duration of the test. **D,** Size of glycolytic response to PMA was calculated as the difference between the basal glycolysis and glycolytic capacity. Statistical difference was assessed using the Friedman test (n = 8). *CTL*, Untreated control; 2-*DG*, 2-Deoxy-D-glucose; *Oligo*, oligomycin; *PER*, proton efflux rate.

Previous studies have investigated the effect of e-cigarette exposure on neutrophil functions, but this is the first to use a model of direct vapor exposure. This study's strength is the comparison of the impact of nicotine on function and phenotype. Our holistic approach in assessing neutrophil function after e-cigarette vapor challenge has captured the broad suppression, which is nicotine-independent as opposed to previously reported nicotine-dependent effects in alveolar macrophages[40,41] and epithelial cells.[42] Nicotine-independent effects are driven by the RCS element consisting of aldehydes, acrolein, and volatile organic compounds, which have been extensively analyzed.[12-15] We chose to standardize the components used by all users—by testing the fundamental e-liquid components of PG, VG, and nicotine, presenting a best possible model and avoiding the need to create intermediate e-cigarette–derived reagents. A limitation of this work is the focus on free-base nicotine e-liquid. Nicotine salt-based e-liquids have gained significant popularity in some regions; however, no differences in biological activity have been demonstrated to date beyond uptake rate across the epithelial barrier.

The direct translation of these findings to *in vivo* effects is limited because each e-cigarette user has their own unique combination of device, e-liquid, and usage pattern. We measured the impact of the base components on neutrophil functions, but the contribution of puff number, flavorings, and device types cannot be confirmed by this work. We have presented here a chamber that will mimic a human lung during vaping. We have previously shown that vaping acts a proinflammatory insult to cells within the lung, such as alveolar macrophages.[41] This causes the release of chemokines that will attract neutrophils from the periphery into the lung where such a direct exposure would occur. This work contrasts with much of the literature to date that focused on the effects of high levels of nicotine exposure or longer duration whole-body exposure in murine studies. We have used a low-dose exposure to yield insight into the effects of physiological exposure in the acute phase of vaping.

This study has used primary neutrophils isolated from healthy nonsmokers to preclude the previous influence of cigarette smoking as a confounding factor in observed results. Primary neutrophils are short-lived after isolation. Therefore, assessing

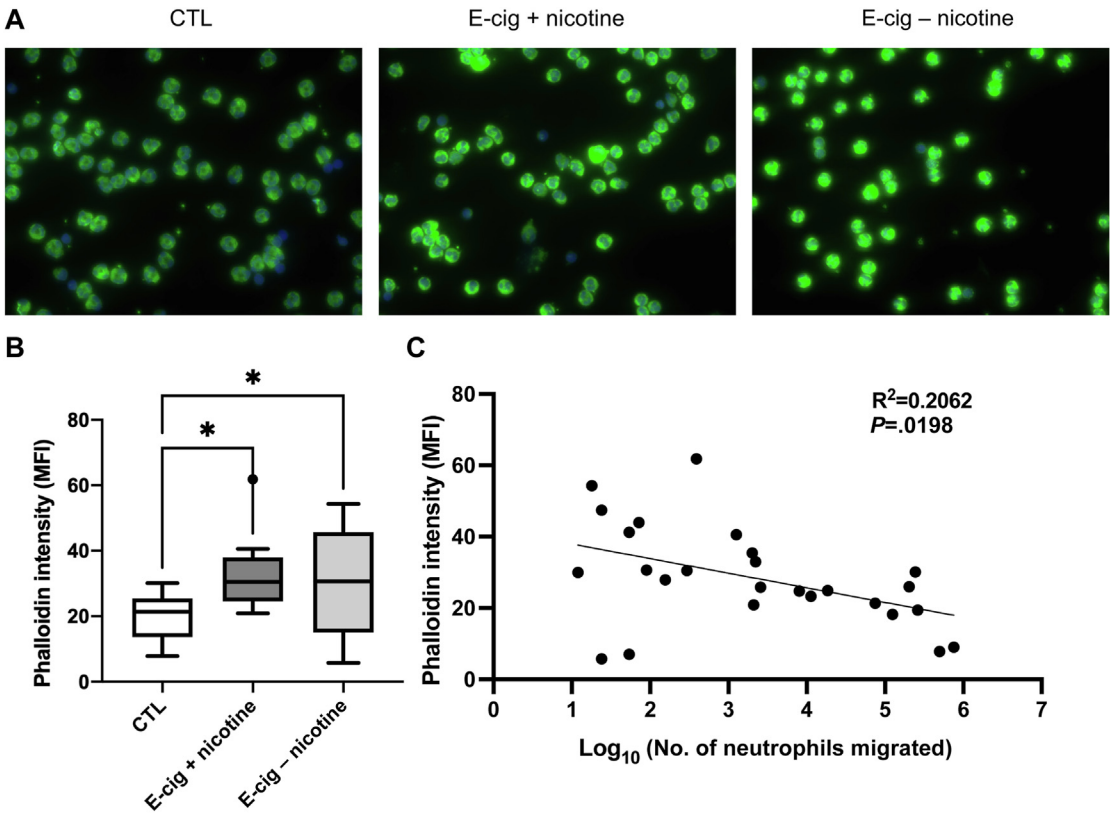

FIG 7. E-cigarette vapor induces actin polymerization in neutrophils. Neutrophils were treated with e-cigarette vapor and stained for polymerized F-actin using phalloidin-FITC with DAPI costaining. **A,** Representative microscopy images, with *green* representing F-actin stained and *blue* representing the nucleus stained with DAPI. **B,** The average fluorescence intensity of 5 fields of view was calculated. **C,** Paired Transwell migration to 100 nM IL-8 was performed, and the ability of neutrophils to migrate, plotted as the log of total neutrophils migrated through the Transwell membrane, was plotted against the phalloidin fluorescence intensity. Statistical difference was calculated using a repeated-measures ANOVA and simple linear regression (n = 9 independent donors). *CTL*, Untreated control; *DAPI*, 4′-6-diamidino-2-phenylindole. $^*P \leq .05$

chronic exposure was not possible. Despite these limitations, our demonstration of significant dysfunction after acute, nontoxic exposure may have long-term consequences. The impact of vaping on lung health is likely to take decades to manifest in histologic abnormalities and even longer for symptoms. To fully characterize how different vaping behaviors affect cellular functions, long-term longitudinal studies will be needed. Until these cohort studies are undertaken, direct exposure systems such as those identified here can be used to further investigate the molecular drivers of cellular dysfunction to understand whether harm can be prevented or reduced. Future work should focus on the individual e-cigarette vapor components driving phenotypic and functional changes in immune and structural cells of the respiratory system.

We have demonstrated changes in neutrophil phenotype and suppression of key neutrophil effector functions. These changes are not nicotine-dependent and are driven by excessive F-actin accumulation in the cytoplasm. The changes observed here mimic some of the neutrophil dysfunctions seen in disease states such as COPD and have the potential to drive persistent inflammation and tissue damage *in vivo*. As such, there are implications for long-term use of e-cigarettes and for derivative devices such as wellness vapes. Although longitudinal research is needed to understand the full extent of the health effects of e-cigarettes, this work adds to the evidence challenging the perception that e-cigarettes are safe and cautions against the emerging trend of long-term e-cigarette usage.

DISCLOSURE STATEMENT

This study was supported by grants from the Dunhill Medical Trust (grant no. RTF1906\86 to D.R.T., A.S., E.S., and F.S.G.); Alpha One Foundation (grant no. 617303) and Health Data Research UK (grant no. NIHR129593) (both to E.S.); Asthma + Lung UK (grant nos. MCFPHD20F\2 and PPRG16 to A.S., D.R.T., and E.S.); Efficacy and Mechanism Evaluation (grant no. NIHR131600), Health Technology Assessment (grant no. NIHR129593), and Medical Research Council (grant no. MR/S002782/1) (all to A.S., D.R.T., E.S., and D.P.); Birmingham Health Partners (to D.P. and D.R.T.); National Institute for Health Research (NIHR) Surgical Reconstruction and Microbiology Research Centre (to J.H.); and Wellcome Trust (grant no. 2Z0180/Z/30/Z to L.C.D.).

Disclosure of potential conflict of interest: The authors declare that they have no relevant conflicts of interest.

We thank Prof Robert Insall for his chemotaxis chamber that has been used in this study.

Key messages

- **Neutrophils exhibit an altered phenotype and are unable to function normally after direct exposure to e-cigarette vapor, independent of nicotine content.**
- **These functional defects are driven by the accumulation of filamentous actin in the cytoplasm.**

REFERENCES

1. Global State of Tobacco Harm Reduction (GSTHR). 82 million vapers worldwide in 2021: the GSTHR estimate. Available at: https://gsthr.org/briefing-papers/82-million-vapers-worldwide-in-2021-the-gsthr-estimate/. Accessed February 1, 2022.
2. McNeill A, Simonavičius E, Brose L, Taylor E, East K, Zuikova E, et al. Nicotine vaping in England: 2022 evidence update including health risks and perceptions. London: Office for Health Improvement and Disparities; 2022.
3. Thompson AB, Daughton D, Robbins RA, Ghafouri MA, Oehlerking M, Rennard SI. Intraluminal airway inflammation in chronic bronchitis. Characterization and correlation with clinical parameters. Am Rev Respir Dis 1989;140:1527-37.
4. Pilette C, Colinet B, Kiss R, André S, Kaltner H, Gabius HJ, et al. Increased galectin-3 expression and intra-epithelial neutrophils in small airways in severe COPD. Eur Respir J 2007;29:914-22.
5. Donaldson GC, Seemungal TA, Patel IS, Bhowmik A, Wilkinson TM, Hurst JR, et al. Airway and systemic inflammation and decline in lung function in patients with COPD. Chest 2005;128:1995-2004.
6. Parr DG, White AJ, Bayley DL, Guest PJ, Stockley RA. Inflammation in sputum relates to progression of disease in subjects with COPD: a prospective descriptive study. Respir Res 2006;7:136.
7. Sapey E, Stockley JA, Greenwood H, Ahmad A, Bayley D, Lord JM, et al. Behavioral and structural differences in migrating peripheral neutrophils from patients with chronic obstructive pulmonary disease. Am J Respir Crit Care Med 2011;183:1176-86.
8. Stringer KA, Tobias M, O'Neill HC, Franklin CC. Cigarette smoke extract-induced suppression of caspase-3-like activity impairs human neutrophil phagocytosis. Am J Physiol Lung Cell Mol Physiol 2007;292:L1572-9.
9. Lee J, Taneja V, Vassallo R. Cigarette smoking and inflammation: cellular and molecular mechanisms. J Dent Res 2012;91:142-9.
10. Keskitalo E, Varis L, Bloigu R, Kaarteenaho R. Bronchoalveolar cell differential count and the number of asbestos bodies correlate with survival in patients with asbestosis. Occup Environ Med 2019;76:765-71.
11. Wells AU, Hansell DM, Haslam PL, Rubens MB, Cailes J, Black CM, et al. Bronchoalveolar lavage cellularity: lone cryptogenic fibrosing alveolitis compared with the fibrosing alveolitis of systemic sclerosis. Am J Respir Crit Care Med 1998;157:1474-82.
12. Kosmider L, Sobczak A, Fik M, Knysak J, Zaciera M, Kurek J, et al. Carbonyl compounds in electronic cigarette vapors: effects of nicotine solvent and battery output voltage. Nicotine Tob Res 2014;16:1319-26.
13. Jensen RP, Luo W, Pankow JF, Strongin RM, Peyton DH. Hidden formaldehyde in e-cigarette aerosols. N Engl J Med 2015;372:392-4.
14. Ogunwale MA, Li M, Ramakrishnam Raju MV, Chen Y, Nantz MH, Conklin DJ, et al. Aldehyde detection in electronic cigarette aerosols. ACS Omega 2017;2:1207-14.
15. Goniewicz ML, Knysak J, Gawron M, Kosmider L, Sobczak A, Kurek J, et al. Levels of selected carcinogens and toxicants in vapour from electronic cigarettes. Tob Control 2014;23:133-9.
16. Corriden R, Moshensky A, Bojanowski CM, Meier A, Chien J, Nelson RK, et al. E-cigarette use increases susceptibility to bacterial infection by impairment of human neutrophil chemotaxis, phagocytosis, and NET formation. Am J Physiol Cell Physiol 2020;318:C205-14.
17. Higham A, Rattray NJ, Dewhurst JA, Trivedi DK, Fowler SJ, Goodacre R, et al. Electronic cigarette exposure triggers neutrophil inflammatory responses. Respir Res 2016;17:56.
18. Reidel B, Radicioni G, Clapp PW, Ford AA, Abdelwahab S, Rebuli ME, et al. E-cigarette use causes a unique innate immune response in the lung, involving increased neutrophilic activation and altered mucin secretion. Am J Respir Crit Care Med 2018;197:492-501.
19. Kumar S, Dikshit M. Metabolic insight of neutrophils in health and disease. Front Immunol 2019;10:2099.
20. Jepsen LV, Skottun T. A rapid one-step method for the isolation of human granulocytes from whole blood. Scand J Clin Lab Invest 1982;42:235-8.
21. Hughes MJ, McGettrick HM, Sapey E. Importance of validating antibody panels: anti-PD-L1 clone binds AF700 fluorophore. J Immunol Methods 2020;483:112795.
22. Hua M, Yip H, Talbot P. Mining data on usage of electronic nicotine delivery systems (ENDS) from YouTube videos. Tob Control 2013;22:103-6.
23. Robinson RJ, Hensel EC, Morabito PN, Roundtree KA. Electronic cigarette topography in the natural environment. PLoS One 2015;10:e0129296.
24. Farsalinos KE, Romagna G, Tsiapras D, Kyrzopoulos S, Voudris V. Evaluation of electronic cigarette use (vaping) topography and estimation of liquid consumption: implications for research protocol standards definition and for public health authorities' regulation. Int J Environ Res Public Health 2013;10:2500-14.
25. Dautzenberg B, Bricard D. Real-time characterization of e-cigarettes use: the 1 million puffs study. J Addict Res Ther 2015;2015:1-5.
26. Pullan J, Greenwood H, Walton GM, Stockley RA, Sapey E. Neutrophil extracellular traps (NETs) in COPD: a potential novel mechanism for host damage in acute exacerbations. Eur Respir J 2015;46:PA5055.
27. Thiam HR, Wong SL, Qiu R, Kittisopikul M, Vahabikashi A, Goldman AE, et al. NETosis proceeds by cytoskeleton and endomembrane disassembly and PAD4-mediated chromatin decondensation and nuclear envelope rupture. Proc Natl Acad Sci U S A 2020;117:7326-37.
28. Singh NR, Johnson A, Peters AM, Babar J, Chilvers ER, Summers C. Acute lung injury results from failure of neutrophil de-priming: a new hypothesis. Eur J Clin Invest 2012;42:1342-9.
29. Ekpenyong AE, Toepfner N, Chilvers ER, Guck J. Mechanotransduction in neutrophil activation and deactivation. Biochim Biophys Acta 2015;1853:3105-16.
30. Jaumouillé V, Waterman CM. Physical constraints and forces involved in phagocytosis. Front Immunol 2020;11:1097.
31. Stroka KM, Hayenga HN, Aranda-Espinoza H. Human neutrophil cytoskeletal dynamics and contractility actively contribute to trans-endothelial migration. PLoS One 2013;8:e61377.
32. Bengtsson T, Jaconi ME, Gustafson M, Magnusson KE, Theler JM, Lew DP, et al. Actin dynamics in human neutrophils during adhesion and phagocytosis is controlled by changes in intracellular free calcium. Eur J Cell Biol 1993;62:49-58.
33. Ghosh A, Coakley RD, Ghio AJ, Muhlebach MS, Esther CR Jr, Alexis NE, et al. Chronic e-cigarette use increases neutrophil elastase and matrix metalloprotease levels in the lung. Am J Respir Crit Care Med 2019;200:1392-401.
34. Reznick AZ, Cross CE, Hu ML, Suzuki YJ, Khwaja S, Safadi A, et al. Modification of plasma proteins by cigarette smoke as measured by protein carbonyl formation. Biochem J 1992;286:607-11.
35. Grimsrud PA, Xie H, Griffin TJ, Bernlohr DA. Oxidative stress and covalent modification of protein with bioactive aldehydes. J Biol Chem 2008;283:21837-41.
36. Barth BM, Stewart-Smeets S, Kuhn TB. Proinflammatory cytokines provoke oxidative damage to actin in neuronal cells mediated by Rac1 and NADPH oxidase. Mol Cell Neurosci 2009;41:274-85.
37. Drost EM, MacNee W. Potential role of IL-8, platelet-activating factor and TNF-alpha in the sequestration of neutrophils in the lung: effects on neutrophil deformability, adhesion receptor expression, and chemotaxis. Eur J Immunol 2002;32:393-403.
38. Lokwani R, Wark PA, Baines KJ, Fricker M, Barker D, Simpson JL. Blood neutrophils in COPD but not asthma exhibit a primed phenotype with downregulated CD62L expression. Int J Chron Obstruct Pulmon Dis 2019;14:2517-25.
39. Friedrichs B, Neumann U, Schüller J, Peck MJ. Cigarette-smoke-induced priming of neutrophils from smokers and non-smokers for increased oxidative burst response is mediated by TNF-α. Toxicol In Vitro 2014;28:1249-58.
40. Ween MP, Whittall JJ, Hamon R, Reynolds PN, Hodge SJ. Phagocytosis and inflammation: exploring the effects of the components of e-cigarette vapor on macrophages. Physiol Rep 2017;5:e13370.
41. Scott A, Lugg ST, Aldridge K, Lewis KE, Bowden A, Mahida RY, et al. Pro-inflammatory effects of e-cigarette vapour condensate on human alveolar macrophages. Thorax 2018;73:1161.
42. Garcia-Arcos I, Geraghty P, Baumlin N, Campos M, Dabo AJ, Jundi B, et al. Chronic electronic cigarette exposure in mice induces features of COPD in a nicotine-dependent manner. Thorax 2016;71:1119-29.

METHODS

Neutrophil isolation

Neutrophils were isolated as described previously.[E1] Lithium-heparin anticoagulated whole blood was transferred to centrifuge tubes and gently mixed with sterile 2% dextran in 0.154 M NaCl in a 6:1 ratio (whole blood:dextran). Blood was left to stand for 30 minutes to allow for erythrocyte sedimentation. Percoll was diluted 9:1 (vol/vol) in 1.54 M NaCl to produce an isotonic stock solution. This was further diluted 14:11 in 0.154 M NaCl to produce a 56% Percoll solution or 4:1 in 0.154 M NaCl to produce an 80% Percoll solution. Percoll solutions were prepared fresh on the day of neutrophil isolation and allowed to come to room temperature before layering. Using a sterile fine-tipped pipette (Alpha Labs, Eastleigh, UK), 80% Percoll was layered beneath 56% Percoll in a centrifuge tube to form a discontinuous Percoll density gradient. Immediately after preparation of the density gradient, the buffy coat from the erythrocyte-sedimented whole blood was gently layered on top of the Percoll gradient using a sterile fine-tipped pipette. Gradients were centrifuged at 470*g* for 20 minutes at room temperature, with no brake or acceleration. Following centrifugation, the plasma and PBMC layers were removed and discarded, and the neutrophil layer was aspirated using a sterile fine-tipped pipette and transferred into a fresh, sterile PBS–containing 15-mL centrifuge tube. Cells were centrifuged at 250*g* for 10 minutes at room temperature with full brake and acceleration to form a pellet. Supernatants were discarded and pellets gently resuspended in RPMI 1640 containing 2 mM L-glutamine and supplemented with penicillin-streptomycin (1% wt/wt). A Fast Read 102 (Biosigma, Hampshire, UK) slide was used to assess neutrophil yield and cells were diluted to the appropriate concentration for downstream experiments in the same RPMI 1640, or assay-specific media as specified. Neutrophil purity was assessed by Cytospin (Thermo Shandon, Horsham, UK). Only preparations with a neutrophil purity of more than 90% were used for subsequent assays.

Neutrophil viability

Neutrophils were resuspended at 1×10^6/mL in Annexin V binding buffer (produced by diluting a 10× concentrated buffer solution consisting of 0.2 μM sterile filtered 0.1 M HEPES (pH 7.4), 1.4 M NaCl, and 25 mM $CaCl_2$ with distilled water 1:10) and transferred to ice. Annexin V–FITC stain (BD Biosciences, Berkshire, UK) was added (1:100 dilution) and the cells were left on ice, protected from light, for 20 minutes. Neutrophils were centrifuged at 250*g* for 5 minutes at 4°C with full brake and acceleration, and supernatants were discarded and resuspended in Annexin V binding buffer. Neutrophils were washed twice more before resuspension in 200 μL of Annexin V binding buffer. Immediately before running, propidium iodide was added to the sample 1:100 (vol/vol). Samples were read on a BD FACSvia flow cytometer (BD Biosciences, Berkshire, UK). Proportions of live (viable) (Annexin V^{low} and PI^{low}), early apoptotic (Annexin V^{high} and PI^{low}), late apoptotic (Annexin V^{high} and PI^{high}), and necrotic (Annexin V^{low} and PI^{high}) neutrophils were determined.

Neutrophil migration assays

Insall chamber—Chemotaxis. The neutrophil chemotaxis assay was performed using a modified Dunn chamber, the Insall chamber.[E2] Neutrophils were resuspended at 2×10^6/mL in RPMI 1640. Glass coverslips (Leica Biosystems, Wetzlar, Germany) were handled using inverted forceps and sterilized by submersion in 0.4 M H_2SO_4 followed by twice in distilled water. Sterilized coverslips were coated in 7.5% BSA before 8×10^5 neutrophils (in 400 μL volume) were added to the coverslip. Control neutrophils were left on the benchtop covered by a petri dish for 20 minutes to adhere to the coverslip, whereas e-cigarette vapor–exposed neutrophils were transferred to the vaping chamber on a petri dish lid and exposed to 40 puffs of e-cigarette vapor during the adherence phase. After a 20-minute incubation, coverslips were inverted and placed on the Insall chamber slide. Chemoattractant wells were filled with 100 nM Recombinant Human (rh)-CXCL8 (Bio-techne, Abingdon, UK). The Insall chamber with coverslip was placed onto a Leica DMI 6000B microscope with fitted DFL350 FX camera (Leica, London, UK). The field of vision was filmed for 12 minutes, with an image captured every 20 seconds. Films were analyzed using the manual tracking plugin on FIJI ImageJ before using a preformulated Excel template to generate values for speed, velocity, persistence, and chemotactic index.

Transwell migration. Neutrophils were resuspended at 1×10^6/mL in RPMI 1640 before e-cigarette exposure to allow for consistency in vaping steps. Following vaping, neutrophils were centrifuged at 250*g* for 10 minutes at room temperature with maximum brake and acceleration and resuspended at 1×10^7/mL. Meanwhile, 600 μL RPMI (phenol red–free + Glutamine-Penicillin-Streptomycin + 10% FCS) was added to required wells of a 24-well plate, which was transferred to an incubator (37°C, 5% CO_2). rh-CXCL8 (100 nM) was added to relevant wells before Nunc Transwell inserts with 3-μm pores (Fisher Scientific, Loughborough, UK; product no. 40627) were placed in the wells. Neutrophils (1×10^6) were transferred to the inserts, and the plate incubated (37°C, 5% CO_2) for 90 minutes. Following the incubation step, inserts were removed and the number of cells in the supernatant measured on a BD FACSvia machine (BD Biosciences, Wokingham, UK).

Neutrophil phagocytosis of *E coli* and *S aureus*

Neutrophils were resuspended at 1×10^6/mL in RPMI 1640. Neutrophils (1×10^5) were then added to each of the required wells of a 96-well flexi-plate that had been precoated with PBS containing 1% BSA. Cytochalasin D (final concentration, 20 μM) was added to negative control neutrophils for 20 minutes; meanwhile, experimental neutrophils were exposed to 40 e-cigarette vapor puffs via the vaping chamber. *S aureus* and *E coli* pHrodo green bioparticles (Thermo Fisher Scientific, Loughborough, UK) were resuspended in pHrodo buffer (Hanks' balanced salt solution, with additional 20 mM HEPES [476.6 mg HEPES in 100 mL Hanks' balanced salt solution] pH adjusted to 7.4 with NaOH to minimize background signal from uningested particles) (made up to 1 mg/mL) and sonicated for 10 minutes to ensure an even suspension. pHrodo bioparticles (50 μL) were added to required neutrophil wells for 30 and 60 minutes and left to incubate at 37°C in 5% CO_2. Negative control neutrophils were incubated with pHrodo bioparticles for 60 minutes. After incubation was complete, plates were transferred to ice to quench phagocytosis before wells were topped up with ice-cold PBS containing 1% BSA. Plates were centrifuged (250*g* for 5 minutes at 4°C with maximum brake and acceleration) and washed

in ice-cold PBS containing 1% BSA twice before being resuspended in PBS containing 1% BSA and transferred to FACS tubes ready for analysis. The BD FACSvia flow cytometer (BD Biosciences) was used for flow-cytometry analysis.

Neutrophil NETosis assays

Immunofluorescence staining for NETs. Neutrophils (2×10^5) were seeded onto glass coverslips (Leica Biosystems, Wetzlar, Germany) in a 6-well plate and incubated at 37°C in 5% CO_2 for 30 minutes. Coverslips were then flooded with RPMI 1640 and 25 nM PMA was added. Plates were returned to the incubator (37°C, 5% CO_2) for 3 hours. Postincubation, 4% paraformaldehyde was added to fix the cells and the plate was incubated (37°C, 5% CO_2) for a further 30 minutes. Coverslips were washed with PBS and then with 0.1% Triton X-100 made up in PBS. Coverslips were washed again 3 times with PBS before staining with 1 μM SYTOX Green (Thermo Fisher Scientific, Loughborough, UK) made up in PBS. Coverslips were washed for a final time with PBS for 5 minutes before being mounted onto microscope slides (Thermo Fisher Scientific) using fluoromount medium (Thermo Fisher Scientific and visualized using the Leica DMI 6000B microscope.

Quantification of NET release. Neutrophils (2×10^5) were added to each well of a 96-well flat-bottom clear plate. Cells were stimulated with 25 nM PMA (or vehicle control) for 3 hours in an incubator (37°C, 5% CO_2). Poststimulation, supernatants were transferred to eppendorfs and centrifuged at 2200*g* for 10 minutes at 4°C. Supernatant of 100 μL was transferred to a flat-bottom 96-well black plate and stained with 1 μM SYTOX Green made up in PBS for 10 minutes at room temperature in the dark. Fluorescence was measured using the BioTek Synergy 2 fluorometric plate reader (Agilent, Milton Keynes, UK) with excitation and emission set at 485/20 nm and 528/20 nm, respectively.

Neutrophil metabolic assay

Agilent Seahorse XF96 analyzers were used to perform metabolic tests. On the day preceding an assay, Seahorse XF96 Cell Culture Microplates (Agilent Technologies, Milton Keynes, UK) were coated with Corning CellTak (Thermo Fisher Scientific) (22.4 μg/mL diluted in 0.1 M $NaHCO_3$ [pH 8.0]) by applying 25 μL to each well and left for 20 minutes at room temperature before washing each well twice with double distilled (dd)H_2O. Plates were stored at 4°C overnight and warmed to 37°C in a non-CO_2 incubator on the morning of the assay. In addition, on the day before the assay, Seahorse XFe96 sensor cartridges (Agilent Technologies) were hydrated by adding ddH_2O to the utility plate and lowering the sensory cartridge into the wells. The assembled sensor cartridge was placed at 37°C in a non-CO_2 incubator overnight.

On the day of the assay, neutrophils were isolated as described and resuspended at 4 x 10^6/mL in prewarmed phenol red–free RPMI dissolved in 1 L distilled water, supplemented with L-glutamine (2 mM), sodium pyruvate (1 mM), glucose (10 mM), and HEPES (5 mM, pH 7.4, filter sterilized), which will be referred to as Seahorse media. Water was discarded from the utility plate and replaced with 200 μL prewarmed Seahorse XF Calibrant solution (Agilent Technologies). The sensor cartridge was re-placed into the calibrant and incubated in a non-CO_2 (37°C) incubator for 45 to 60 minutes. Meanwhile, 50 μL neutrophil solution was loaded into experimental wells of the CellTak-coated plate and 50 μL Seahorse media into background/control wells. The plate was centrifuged at 200*g* for 1 minute with maximum acceleration but no brake at room temperature before incubation in a non-CO_2 (37°C) incubator for 25 to 30 minutes. Warm Seahorse media (130 μL) was gently added down the side of each well, taking care to avoid disturbing the cells. The base of the plate was observed under a light microscope to ensure cells were still adherent, and the plate was transferred back to the non-CO_2 (37°C) incubator for a further 15 to 25 minutes. Meanwhile, 25 μL of each inhibitor/stimulant was added to the injection ports A to C of the sensor cartridge, following the loading strategy for glycolysis test (A, 1.6 μM PMA; B, 16 mM oligomycin; C, 500 mM 2-Deoxy-D-glucose [2-DG]) and oxidative burst (A, Seahorse media; B, 20 μM rotenone/antimycin A; C, 1.6 μM PMA). The procedure steps were preset on the protocol template made using the Seahorse Wave Desktop software version 2.6, and analysis was performed using preformatted analysis templates. Extracellular acidification rate was converted to proton efflux rate to account for the buffering capacity of the media.

Neutrophil ROS production

Neutrophils (1×10^5) were added to FACS tubes. CellROX dyes (Invitrogen, Oxford, UK) were used to detect cytoplasmic (red) and mitochondrial/nuclear (green) ROS. CellROX dyes were added at a concentration of 5 mM to relevant tubes and incubated at 37°C in 5% CO_2 for 30 minutes in the dark. Cells were washed twice with PBS (300*g* for 5 minutes at room temperature with full brake and acceleration) before being resuspended in 200 μL PBS. Cells were acquired using a MACSQuant analyzer 10 flow cytometer (Miltenyi Biotec, Bisley, UK). CellROX green was detected on FITC channel, whereas CellROX red was detected on allophycocyanin. Data were analyzed using FlowJo software version 10 (Tree Star, Inc, Ashland, Ore), and the MFI was compared between the groups.

Neutrophil phenotyping

Neutrophils (1×10^5) were added to FACS tubes. Cells were washed with FACS buffer (PBS containing 1% BSA) (300*g* for 5 minutes at room temperature with full brake and acceleration) before Fc block was added using human Trustain FcX (BioLegend, London, UK) diluted 1:100 in FACS buffer for 5 to 10 minutes at room temperature. Neutrophils were washed (300*g* for 5 minutes at room temperature with full brake and acceleration) with 400 μL FACS buffer and resuspended in 100 μL antibody cocktail (see Table E3) for both neutrophil panels and isotype controls. Unstained neutrophils were incubated without antibodies or isotype controls. Neutrophils were incubated on ice for 30 minutes, protected from light. Following incubation, neutrophils were washed with 400 μL FACS buffer (300*g* for 5 minutes at 4°C with full brake and acceleration) and resuspended in 200 μL FACS buffer for acquisition. Acquisition was performed using a BD LSR Fortessa flow cytometer (BD Biosciences) and samples analyzed using FlowJo software (Tree Star, Inc).

F-actin polymerization assessment

After e-cigarette vapor exposure, 1.5×10^5 neutrophils were spun (300*g* for 5 minutes) onto microscopy slides. Slides were fixed by submersion in 4% paraformaldehyde for 10 minutes at room

temperature. Slides were washed 3 times (5 minutes each) in PBS before treatment with 0.2% Triton X-100 for 3 minutes at room temperature. Slides were once again washed 3 times in PBS before submersion for 30 minutes in PBS containing 1% BSA. Slides were washed in PBS and then stained using FITC-conjugated phalloidin (Thermo Fisher Scientific) diluted 1:400 in PBS containing 1% BSA for 1 hour at room temperature, protected from light. Slides were washed 3 times in PBS and then stained with 4'-6-diamidino-2-phenylindole nucleic acid stain diluted 1:10,000 in PBS containing 1% BSA for 2 minutes at room temperature. Slides were washed with PBS for a final time before coverslips (22 × 22 mm) were mounted onto the slides using fluoromount medium. Cells were imaged using a Leica DMI 6000B microscope at 40× magnification. Five fields of view were captured per slide, and the fluorescence was quantified using FIJI ImageJ.

REFERENCES

E1. Jepsen LV, Skottun T. A rapid one-step method for the isolation of human granulocytes from whole blood. Scand J Clin Lab Invest 1982;42:235-8.
E2. Grudzinska FS, Jasper A, Sapey E, Thickett DR, Mauro C, Scott A, et al. Real-time assessment of neutrophil metabolism and oxidative burst using extracellular flux analysis. Front Immunol 2023;14:1083072.
E3. Drost EM, MacNee W. Potential role of IL-8, platelet-activating factor and TNF-alpha in the sequestration of neutrophils in the lung: effects on neutrophil deformability, adhesion receptor expression, and chemotaxis. Eur J Immunol 2002;32:393-403.
E4. Lokwani R, Wark PA, Baines KJ, Fricker M, Barker D, Simpson JL. Blood neutrophils in COPD but not asthma exhibit a primed phenotype with downregulated CD62L expression. Int J Chron Obstruct Pulmon Dis 2019;14:2517-25.
E5. Friedrichs B, Neumann U, Schüller J, Peck MJ. Cigarette-smoke-induced priming of neutrophils from smokers and non-smokers for increased oxidative burst response is mediated by TNF-α. Toxicol In Vitro 2014;28:1249-58.

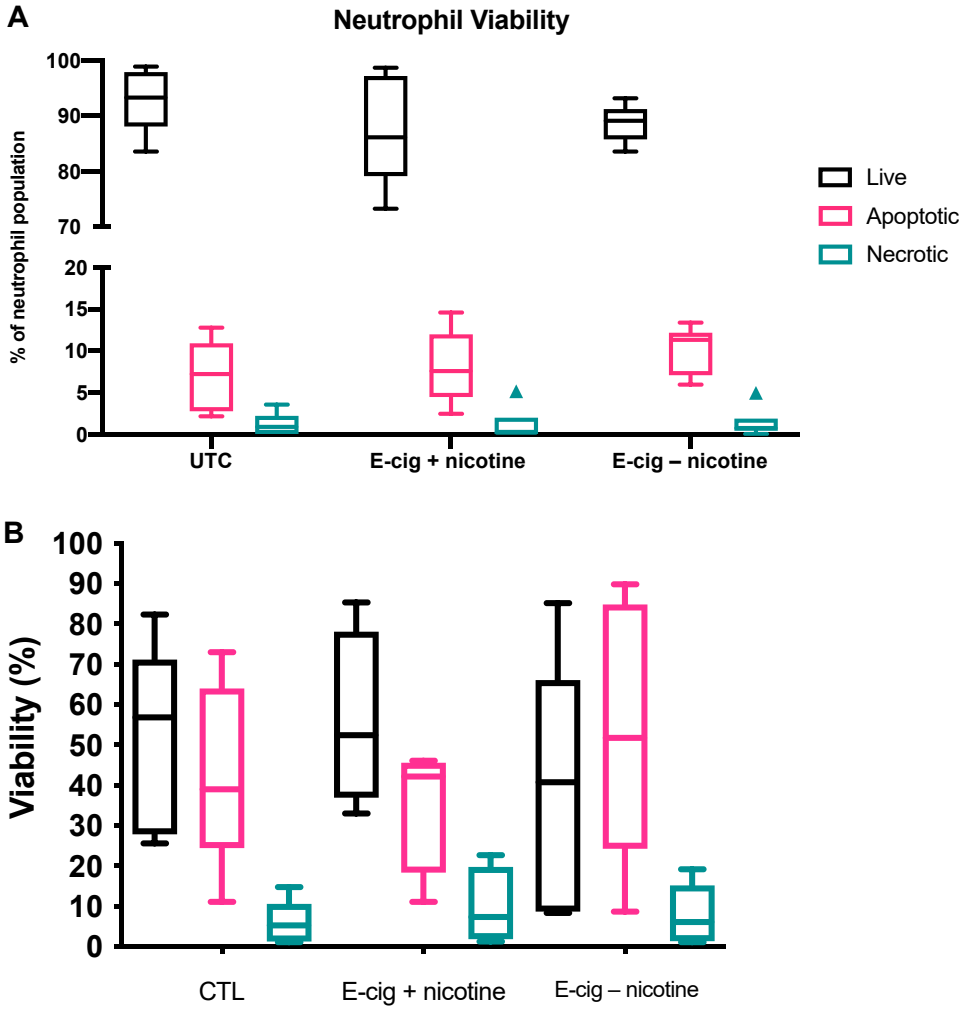

FIG E1. Neutrophil viability after exposure to e-cigarette vapor with and without nicotine **A,** Neutrophils were exposed to e-cigarette vapor for 20 minutes and then assayed (n = 6). **B,** Neutrophils were exposed to e-cigarette vapor for 20 minutes and then cultured for 24 hours (n = 5) before being stained with Annexin V–FITC and PI to assess viability. Viability was assessed using a flow cytometer. Annexin $V^{-}PI^{-}$ cells were considered live, Annexin $V^{+}PI^{-}$ cells were considered early apoptotic, Annexin $V^{+}PI^{+}$ cells were considered late apoptotic, and Annexin $V^{-}PI^{+}$ cells were considered necrotic. Apoptotic cells are expressed as the sum of early and late apoptotic cells. The Kruskal-Wallis test was performed to assess statistical differences between the groups; there were no statistical differences. *CTL*, Untreated control; *PI*, propidium iodide; *UTC*, untreated control.

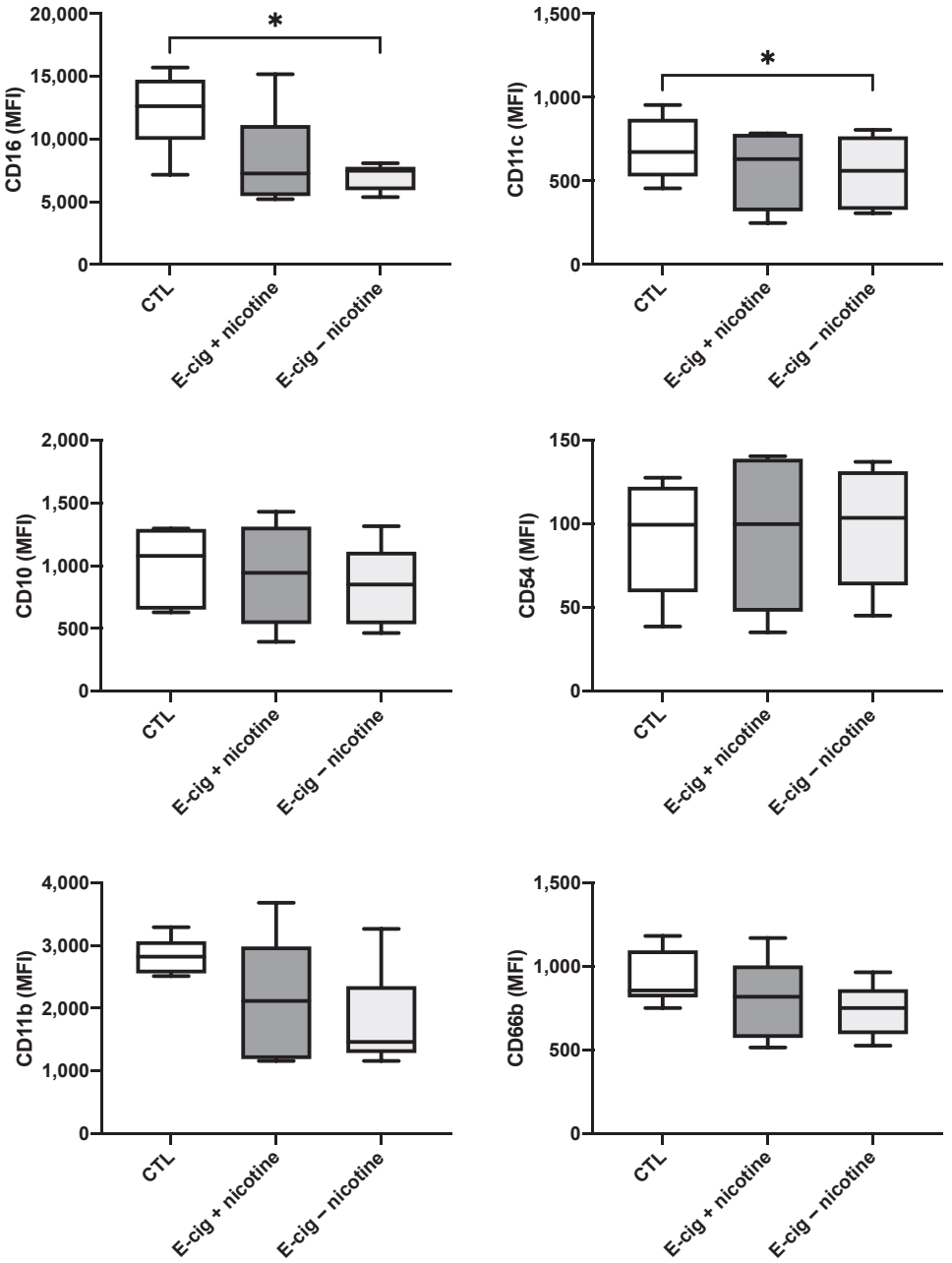

FIG E2. Neutrophil surface marker phenotyping after e-cigarette vapor exposure. Neutrophils were treated with e-cigarette vapor as described, and the expression of 11 surface markers was measured using a multicolor panel and analyzed using a flow cytometer. The expression of each marker is expressed as the MFI. Statistical significance was assessed using the Friedman test. A significant difference between treatment groups is indicated by asterisks above a capped line between the 2 statistically different groups. *CTL*, Untreated control. $*P \leq .05$ (n = 6).

TABLE E1. Neutrophil phenotypic marker and functional measurements contributing to this study

Measure	CTL		E-cigarette + nicotine			E-cigarette − nicotine			*P* value between treatments
	Median	IQR	Median	IQR	*P* value	Median	IQR	*P* value	
Live cells (% of total)	93.3	9.83	89.51	5.47	>.9999	86.51	18.05	.6101	>.9999
CD62L (MFI)	11,651	2,483	3,309	3,503	.0045*	3308	3503	.1299	.7446
CXCR2 (MFI)	3,394	1,096	1,786	1,479.5	.0045*	2698	756	.1299	.7446
CD184 (MFI)	410.5	85.8	296	132.2	.0628	251.5	57.5	.0117*	>.9999
CD11c (MFI)	673.5	345	631	464	.0628	560.5	440.5	.0117*	>.9999
CD16 (MFI)	12,618	4,798	7,263	5,659	.0628	7,476	1,867	.0117*	>.9999
PD-L1 (MFI)	97.05	63.25	147	163.82	.4467	46.2	47.25	.1818	.0027*
CD10 (MFI)	1,079	644	942	776.2	.2498	850	578.2	.2498	>.9999
CD54 (MFI)	99.40	63.2	99.85	91.45	>.9999	103.6	68.25	.2498	>.9999
CD66b (MFI)	855.9	281.6	817.8	433.5	.4467	750.8	269.2	.1299	>.9999
Transwell (no. of neutrophils migrated)	293,442	248,887	666	220,104	.0032*	1,071	262,622	.0203*	>.9999
Chemokinesis (μm/min)	2.864	1.11	1.00	1.27	.0058*	0.87	1.27	.0152*	>.9999
Chemotaxis (μm/min)	0.53	0.81	−0.03	0.25	.0433*	−0.006	0.54	.0853	>.9999
30-min phagocytosis of *E coli* pHrodo bioparticles (% positive)	65.74	34.90	3.71	30.90	.0060*	1.42	30.30	.0026*	>.9999
60-min phagocytosis of *E coli* pHrodo bioparticles (% positive)	90.31	11.67	3.44	73.48	.0157*	1.72	34.87	.0034*	>.9999
30-min phagocytosis of *S aureus* pHrodo bioparticles (% positive)	71.46	28.16	4.77	12.99	.0044*	5.57	10.23	.0021*	>.9999
60-min phagocytosis of *S aureus* pHrodo bioparticles (% positive)	92.50	7.08	5.20	65.72	.0044*	8.25	36.54	.0021*	>.9999
Unstimulated NETosis (RFU)	2,535	1,289	2,283	1,998	>.9999	2,058	1,749	.6339	.9519
NET response to PMA (ΔRFU)	1,153	1,142.3	161.5	1,234	.0226*	116	455	.0099*	>.9999
Oxidative burst response (pmol O_2)	10,643	8,422	2,492	4,600.2	.0056*	3,222	5,790	.0189*	>.9999
Cytoplasmic ROS (MFI)	114.5	58.12	12.49	20.19	.0628	5.91	16.35	.0117*	>.9999
Nuclear/mitochondrial ROS (MFI)	29.85	15.15	5.57	2.33	.0911	4.71	0.88	.0073*	>.9999
Basal glycolysis (PER)	43.26	70.86	73.94	52.54	>.9999	36.26	36.61	>.9999	.6478
Stimulated glycolysis (PER)	259.3	109.6	120.4	210.87	.2141	111.3	243.09	.1687	>.9999
F-actin polymerization (MFI)	21.37	11.8	30.51	13.41	.0237*	30.66	30.68	.0360*	.9636

Neutrophil surface marker expression and a range of effector functions were measured as part of this study. The median and IQR values for treated (e-cigarette + nicotine and e-cigarette − nicotine) and untreated (CTL) are displayed, along with the corresponding *P* value, which represents the significance level between untreated and corresponding treatment groups. Statistical significance was calculated using repeated-measures ANOVA, the Friedman test, and the Kruskal-Wallis test of statistical difference.

CD, Cluster of differentiation; *CTL*, untreated control; *CXCR*, C-X-C chemokine receptor; *IQR*, interquartile range; *PD-L1*, programmed death ligand 1; *PER*, proton efflux rate; *RFU*, relative fluorescence unit.

*$P < .05$ was considered statistically significant.

TABLE E2. Summary table of reported changes in CD62L after stimulation

Donor	Stimuli	Fold reduction in CD62L MFI	Reference
Healthy volunteers	E-cigarette vapor + nicotine 20 min	90.6%	This study
Healthy volunteers	E-cigarette vapor without nicotine 20 min	71.6%	This study
Healthy volunteers	100 nM fMLP 10 and 30 min	50% at 10 min 60% at 30 min	E3
Healthy volunteers	10 nM PAF 10 and 30 min	20% at 10 min 40% at 30 min	E3
Healthy volunteers	10 ng/mL CXCL8 10 and 30 min	Zero at 10 min 20% at 30 min	E3
Healthy volunteers	5 ng/mL TNF-α 10 and 30 min	Zero at 10 min 20% at 30 min	E3
Healthy volunteers	10 and 100 nM fMLP	30% at 10 nM 40% at 100 nM	E4
Patients with COPD	10 and 100 nM fMLP	35% at 10 nM 35% at 100 nM	E4
Healthy volunteers (smokers)	Cigarette smoke–bubbled PBS at 0.12 puffs/mL 30 min	80% reduction in smokers	E5
Healthy volunteers (nonsmokers)	Cigarette smoke–bubbled PBS at 0.12 puffs/mL 30 min	60% reduction in nonsmokers	E5

Table comparing data from this study with the published literature, reporting change in surface expression of the neutrophil lection CD62L, following challenge with e-cigarette vapor, cigarette smoke extract, fMLP, PAF, TNF-α, and CXCL8.
fMLP, N-Formylmethionine-leucyl-phenylalanine; *PAF*, platelet-activating factor.

TABLE E3. Antibodies* used for neutrophil phenotyping

Panel	Receptor	Catalyst no.	Fluorophore	Dilution
Panel 1	CD184	306518	BV421	1:20
	CD10	312220	BV510	1:20
	CD62L	304834	BV605	1:100
	CD11b	301346	BV786	1:40
	CXCR2	320704	FITC	1:40
	CD54	322712	APC	1:100
	CD16	302026	AF700	1:40
Panel 2	PD-L1	329724	BV605	1:100
	CD11c	371516	FITC	1:40
	CD66b	305118	APC	1:100

APC, Allophycocyanin.
*All were purchased from BioLegend.